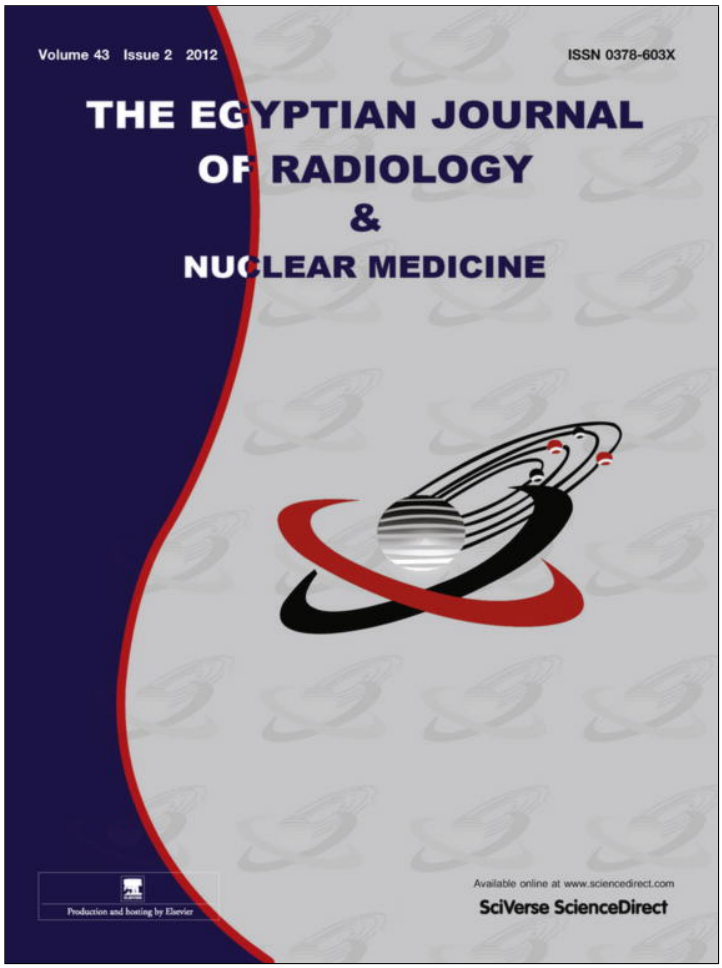

The Egyptian Journal of Radiology and Nuclear Medicine (2012) **43**, 219–226

Egyptian Society of Radiology and Nuclear Medicine

The Egyptian Journal of Radiology and Nuclear Medicine

www.elsevier.com/locate/ejrnm
www.sciencedirect.com

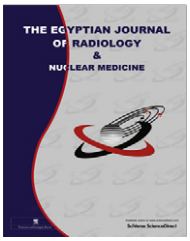

ORIGINAL ARTICLE

Diagnostic impact of echo planar diffusion-weighted magnetic resonance imaging (DWI) in musculoskeletal neoplastic masses using apparent diffusion coefficient (ADC) mapping as a quantitative assessment tool

Sherif Abdelfattah Khedr [a,1], **Mohamed Abdelfattah Hassaan** [a,*], **Naglaa Mohamed Abdelrazek** [a,2], **Amr yehia Sakr** [b,3]

[a] *Radiology Department Cairo University, Egypt*
[b] *Radiotherapy Department Cairo University, Egypt*

Received 4 October 2011; accepted 17 March 2012
Available online 12 April 2012

KEYWORDS

Diffusion-weighted images;
Soft-tissue tumors;
EPI

Abstract *Purpose:* To evaluate the diagnostic impact of echo planar DW imaging in distinguishing benign from malignant musculoskeletal soft-tissue masses using ADC mapping as a quantitative assessment tool.
Patients and methods: We evaluated 73 tumors (21 bone tumors and 52 soft-tissue tumors). MR examinations were performed with a 1.5-T system. Diffusion-weighted single-shot EPI images were obtained in all patients. Apparent diffusion coefficients (ADCs) were calculated by using *b* factors

* Corresponding author. Tel.: +20 105600614.
E-mail addresses: sharifkheder@yahoo.com (S.A. Khedr), moh_a_hassan@yahoo.com (M.A. Hassaan), naglaabdelrazek@yahoo.com (N.M. Abdelrazek), naglaabdelrazek@yahoo.com (A.yehia Abdelrazek).
[1] Tel.: +20 152106961.
[2] Tel.: +20 1449957.
[3] Tel.: +20 101450259.

Peer review under responsibility of Egyptian Society of Radiology and Nuclear Medicine.
http://dx.doi.org/10.1016/j.ejrnm.2012.03.003

ELSEVIER **Production and hosting by Elsevier**

of 0 and 1000 s/mm^2. ADC value measurements were compared with the histopathological findings.
Results: The average ADC of benign tumors was $1.86 \pm 0.67 \times 10^{-3}$ mm^2/s, and that of malignant soft-tissue tumors was $0.97 \pm 0.35 \times 10^{-3}$ mm^2/s. ADC value of malignant tumors was significantly lower than that of the benign tumor group ($p < 0.0001$). The highest ADC value was seen in the case of ganglion cyst ($2.8 \pm 0.23 \times 10^{-3}$ mm^2/s) and cystic neurofibroma ($2.5 \pm 0.04 \times 10^{-3}$ mm^2/s), and juxta cortical enchondroma ($2.65 \pm 0.36 \times 10^{-3}$ mm^2/s) while the lowest one was seen in aggressive fibromatosis ($0.37 \pm 0.05 \times 10^{-3}$ mm^2/s). For malignant soft-tissue masses, the highest ADC value was seen in mesenchymal chondrosarcoma (2.1 ± 0.32) liposarcoma (intermediate grade) (1.4 ± 0.21) while the lowest ADC value was seen in fibrosarcoma (high grade) (0.78 ± 0.14).
Conclusion: MR diffusion provides additional information to the routine MRI sequences rendering it an effective non-invasive tool in differentiating between benign and malignant soft-tissue tumors.

1. Introduction

Diffusion-weighted magnetic resonance imaging (MRI) reflects intra-voxel incoherent motion (IVIM). In biological tissues, motion includes Brownian motion of extra-, intra-, and trans-cellular individual water molecules (true diffusion) as well as microcirculation of blood (perfusion) (1). Both true diffusion and perfusion contribute to the frequently used apparent diffusion coefficient (ADC). Diffusion-weighted MRI has been used successfully in the central nervous system (CNS), especially in the diagnosis of acute stroke (2–4), but also in distinguishing different components of brain tumors (5,6). Diffusion measurements of tumors outside the brain have also been reported. A study of osteogenic sarcoma by Schnapauff et al. (7) indicates that diffusion-weighted MRI can accurately differentiate between viable and necrotic tumor regions. Maier et al. (8) reported quantitative diffusion measurements of breast tumors in mice. Moreover, Baur et al. (9) reported diffusion measurements in human spine that could reliably differentiate acute benign from neoplastic vertebral compression fractures. These studies have demonstrated potential for providing information that can contribute to the differentiation between benign and malignant tumors, and can identify various tumor components (9).

The purpose of this study is to evaluate the diagnostic impact of echo planar DW imaging in distinguishing benign from malignant musculoskeletal soft-tissue masses using ADC mapping as a quantitative assessment tool.

2. Patients and methods

2.1. Patients

From December 2008 to November 2010, we prospectively included 73 consecutive patients (23 females and 50 males; age range 11–70 years; median age 41 years) with clinically suspected musculoskeletal neoplasm. The patients were subjected to clinical examination, previous X-ray and ultrasonography examination. In all patients diagnosis was confirmed after MRI with histologic biopsy and/or examination of the resected specimens. We evaluated 73 tumors (27 bone tumors and 46 soft-tissue tumors).

2.2. MR imaging technique

All patients underwent MRI using a 1.5-T MR system (Magnetom Symphony, Syngo 1.5 T Siemens) with the following pulse sequences.

Standard protocols for musculoskeletal system:

(1) T1WI (TR/TE/NEX; 450/15/1; FOV, 20–30) in axial, coronal and sagittal planes.
(2) Fast spin-echoT2WI (TR/TE/NEX); 3000–3500/100–120/2; FOV, 20–30) in axial, coronal and sagittal planes.
(3) Short inversion recovery (STIR) (TR/TE/TI/NEX); 5000–5300/30–50/160/2; FOV, 20–30) in axial, coronal and sagittal planes.
(4) Gradient recalled echo (GRE)(TR/TE/NEX;700–750/20–30/2; FOV,20–30) with flip angle 15–30° in axial, coronal or sagittal planes.
(5) Post-contrast T1WI SE and T1-fat suppressed images in axial, coronal and sagittal planes using gadolinium D.T.P.A (0.1 mmol/kg body weight).
(6) Diffusion weighted images

A diffusion-weighted spin-echo sequence with peripheral pulse triggering (TR – 2-RR, TE – 70, flip angle – 90°, field of view (FOV) – 200–300 mm, matrix size – 51–128) was used with diffusion gradient strengths yielding five *b* values ranging from 0 to 701 s/mm^2 (*b* – 0, 176, 351, 526, and 701 s/mm^2).

Six slices through the tumor were acquired with a slice thickness of 5 mm and an inter slice gap of 2.5 mm

Body parts containing the tumors were immobilized to prevent motion artifacts.

Arbitrarily shaped regions of interest (ROIs) for data analysis was positioned in tumor on the basis of the T2-weighted reference image (*b* – 0 s/mm^2) and copied to all isotropic images of subsequent *b*-values.

When multiple tumor components (solid vs. cystic) could be identified, measurements were taken in the solid components. The mean signal intensities on five isotropic images obtained with different *b*-values were used to calculate the ADC values.

Differences in ADC values between malignant and benign soft-tissue masses were evaluated using Student's *t*-test. *p* values less than 0.05 were considered a statistically significant.

Table 1 The number and ADC value of benign masses.

Benign lesions	Number	Main ADC value measurements (mm^2/s)
Hemangioma	6	1.4 ± 0.18–$1.6 \pm 0.2 \times 10^{-3}$
Juxtacortical enchondroma	2	$2.65 \pm 0.36 \times 10^{-3}$
Ganglion	7	1.9 ± 0.21–$2.8 \pm 0.23 \times 10^{-3}$
Schwannoma	5	$1.5 \pm 0.19 \times 10^{-3}$
Neurofibroma	3	$1.75 \pm 0.26 \times 10^{-3}$
Cystic neurofibroma	1	$2.5 \pm 0.04 \times 10^{-3}$
Aggressive fibromatosis	2	$0.37 \pm 0.05 \times 10^{-3}$
Osteochondroma	3	$2.1 \pm 0.34 \times 10^{-3}$
Elastofibroma	2	$1.9 \pm 0.24 \times 10^{-3}$
PVN	2	$2.21 \pm 0.14 \times 10^{-3}$
Total	33	$1.86 \pm 0.67 \times 10^{-3}$

Table 2 The number and ADC value of malignant masses.

Malignant Tumors	Number	Main ADC value measurements (mm^2/s)
Low grade sarcoma	6	$1.1 \pm 0.22 \times 10^{-3}$
Intermediate liposarcoma	2	$1.4 \pm 0.21 \times 10^{-3}$
High grade liposarcoma	2	$0.97 \pm 0.18 \times 10^{-3}$
Intermediate fibrosarcoma	3	$1.0 \pm 0.2 \times 10^{-3}$
High grade fibro sarcoma	2	$0.78 \pm 0.14 \times 10^{-3}$
Malignant fibrous histiocytoma	2	$0.81 \pm 0.18 \times 10^{-3}$
Neurofibrosarcoma	1	$0.96 \pm 0.17 \times 10^{-3}$
Metastatic deposits	6	$0.9 \pm 0.18 \times 10^{-3}$
Ewing's sarcoma	4	$1.1 \pm 0.9 \times 10^{-3}$
Giant cell tumor	6	$1.1 \pm 0.5 \times 10^{-3}$
Osteosarcoma	5	$0.9 \pm 0.6 \times 10^{-3}$
Mesenchymal chondrosarcoma	1	$2.1 \pm 0.32 \times 10^{-3}$
Total	40	$0.97 \pm 0.35 \times 10^{-3}$

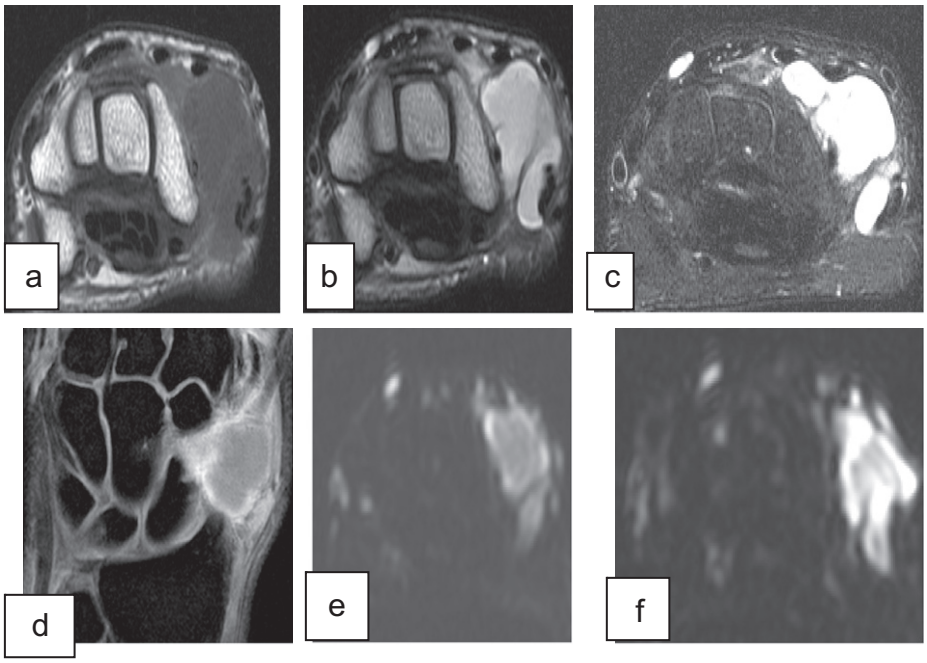

Fig. 1 Ganglion cyst on the lateral aspect of the wrist appears of low signal in axial T1WIs(a), high signal in axial T2WIs and fat suppression sequence (b,c), with no appreciable l contrast enhancement in fat suppression T1WIs(d) . No restriction in DWI(e,f) and ADC. ADC Value 2.8 ± 0.23.

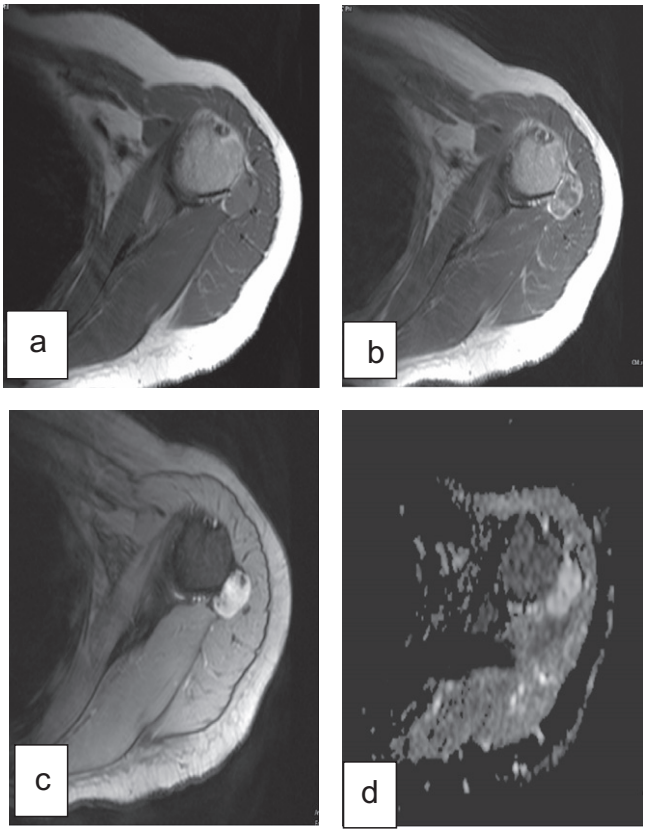

Fig. 2 Juxtacortical Enchondroma of the humeral head appears of low signal in axial T1WIs(a), heterogenous high signal in axial T2WIs and fat suppression sequence (b,c), with No restriction in DWI and ADC (d) ADC Value 2.65 ± 0.36.

3. Results

Seventy-three patients (50 males and 23 females) were included in this study. Their ages range from 11 to 70 years; median age 41 years. The diagnosis of the soft-tissue masses was confirmed with histopathologic examination after excision biopsy (in 61 patients) or post-surgical excision (in 12 patients). 33 masses were benign and 40 masses were malignant. Twenty-one bone tumors and 52 soft-tissue tumors (Tables 1 and 2).

The average ADC of benign cases was $1.86 \pm 0.67 \times 10^{-3}$ mm^2/s, and that of malignant soft-tissue tumors was $0.97 \pm 0.35 \times 10^{-3}$ mm^2/s. ADC value of malignant tumors was significantly lower than that of the benign tumor group ($p < 0.0001$). The highest ADC value was seen in the case of ganglion cyst ($2.8 \pm 0.23 \times 10^{-3}$ mm^2/s) (Fig. 1), juxta cortical enchondroma ($2.65 \pm 0.36 \times 10^{-3}$ mm^2/s) (Fig. 2) and cystic neurofibroma ($2.5 \pm 0.04 \times 10^{-3}$ mm^2/s) (Fig. 3) while the lowest one was seen in aggressive fibromatosis ($0.37 \pm 0.05 \times 10^{-3}$ mm^2/s) (Fig. 4). For malignant soft-tissue masses, the highest ADC value was seen in mesenchymal chondrosarcoma ($2.1 \pm 0.32 \times 10^{-3}$ mm^2/s) and liposarcoma (intermediate grade) (1.4 ± 0.21) (Fig. 5) while the lowest ADC value was seen in fibrosarcoma (high grade) (0.78 ± 0.14) (Fig. 6), GCT (Fig. 7), osteosarcoma (Fig. 8), and Ewing's sarcoma (Fig. 9), showed intermediate ADC.

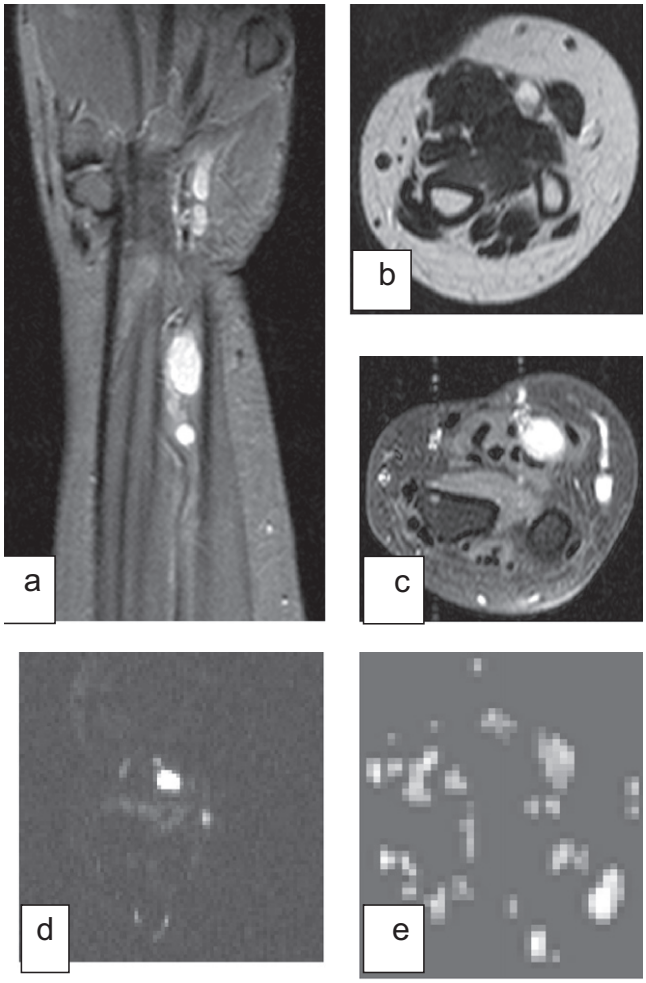

Fig. 3 Cystic Neurofibroma appears of low signal in coronal T1WIs(a), high signal in axial T2WIs and fat suppression sequence (b,c). No restriction in DWI(d,e) and ADC. ADC Value 2.5 ± 0.04.

4. Discussion

Magnetic resonance imaging has an important role in diagnosis, staging and follow-up of soft-tissue masses owing to its precise visualization of degenerative changes, tumor and inflammatory disease.

Tissue contrast attained by using diffusion-weighted magnetic resonance (MR) imaging is different from that attained by using conventional MR techniques. The diffusion technique involves the diffusion motion of water protons in the tissues, and this technique produces different contrast in different kinds of tissue. Therefore, the findings of this procedure can provide different information about diseased tissues (4). Recently DWI was used to characterize soft-tissue tumor, differentiate between benign and malignant soft-tissue masses.

Our results demonstrate increased apparent diffusion coefficients in benign soft-tissue masses compared to malignant soft-tissue masses where the main ADC value of all benign soft-tissue masses was 1.86 ± 0.67 while the main ADC value for all malignant soft-tissue masses was 0.97 ± 0.35. This may be attributed to the increased diffusion of water molecules in

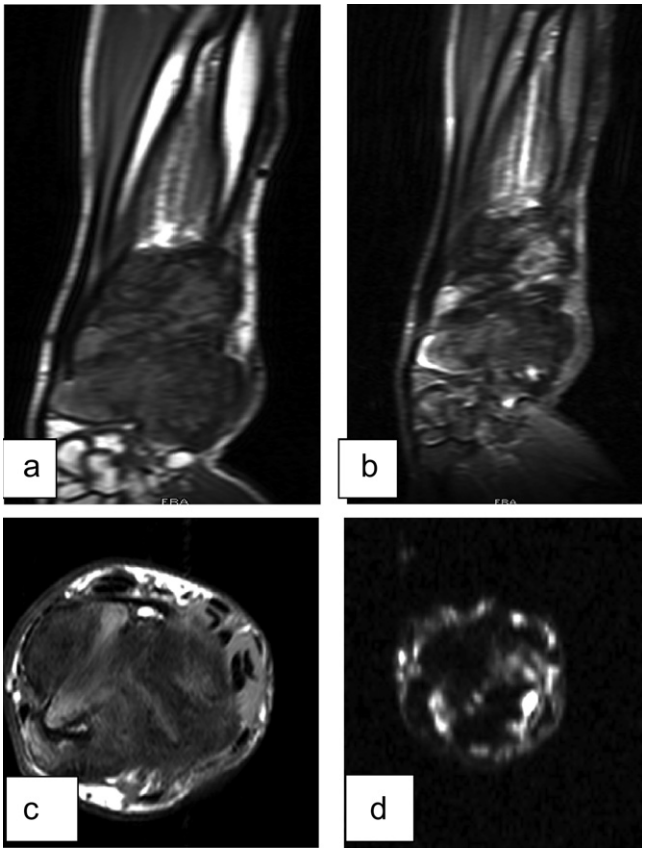

Fig. 4 Aggressive fibromatosis of the ankle appearing of low signal in coronal T1 and T2WIs(a&b) with non uniform contrast enhancement in post contrast axial T1WIs(c) high restriction in ADC(d). ADC Value 0.37 ± 0.05.

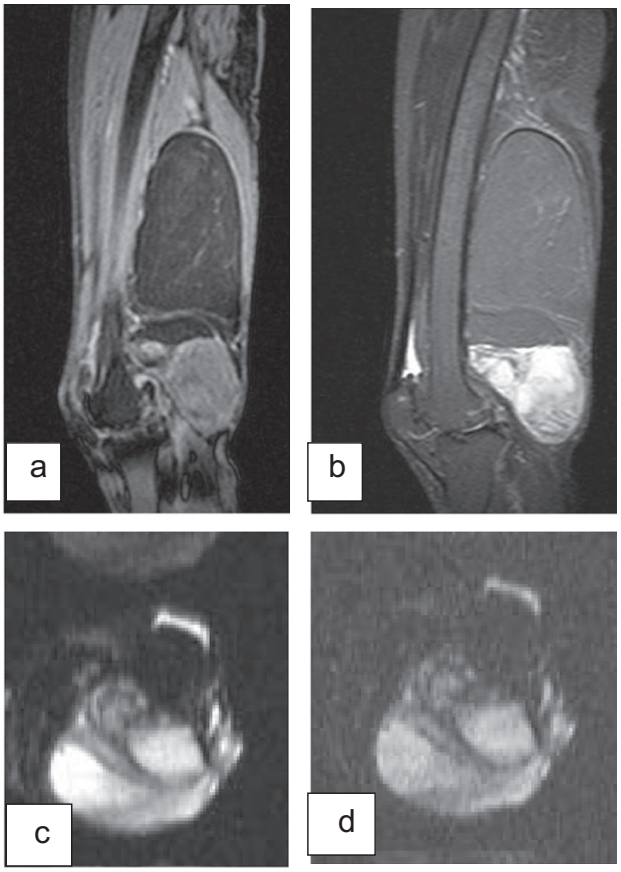

Fig. 6 Liposarcoma of the thigh.The soft tissue component appears of high signal in sagittal fat suppression sequence (a) and intensely enhancing in sagittal T1 fat suppression(b) and showing restriction in DWI(c,d) and ADC . ADC Value 1.1 ± 0. 13.

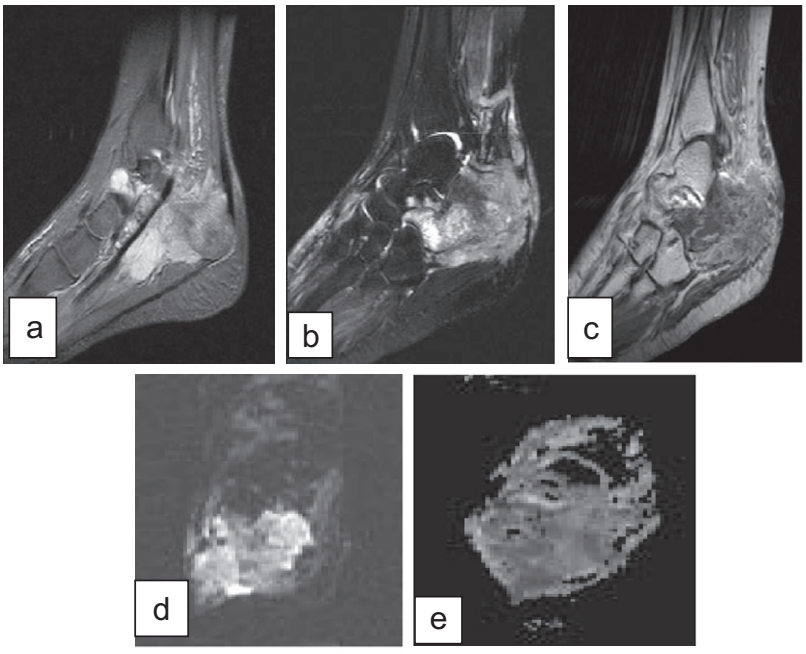

Fig. 5 Mesenchyma chondrosarcoa of the calcaneus appears of high signal in sagittal STIR, T2 fat supression (a,b)) with non uniform contrast enhancement in post contrast sagittal T1WIs. restriction in DWI(d,e) and ADC. ADC Value 2.1 ± 0. 32.

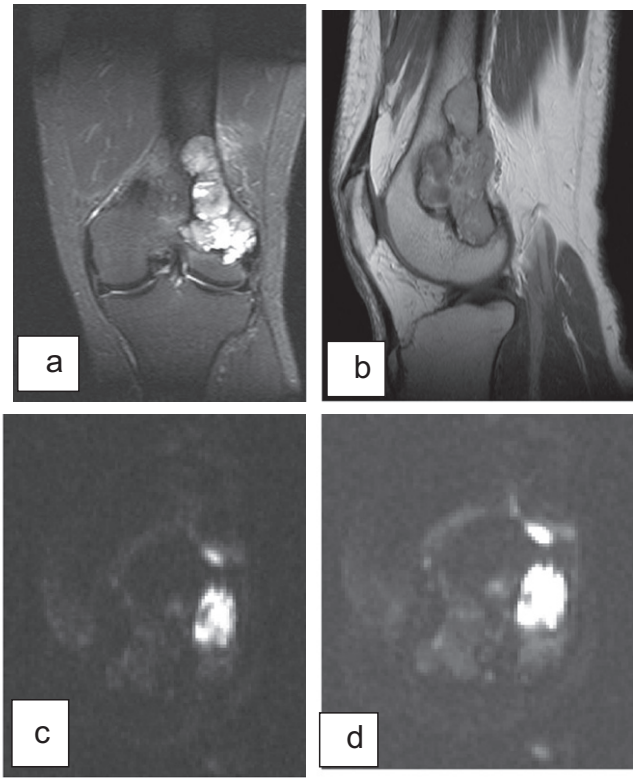

Fig. 7 GCT of the distal femur appears of high signal in coronal fat suppression (a), low signalinn sagittall T1WIs(b). No restriction in DWIc,(d) and ADC. ADC Value 1.2 ± 0.

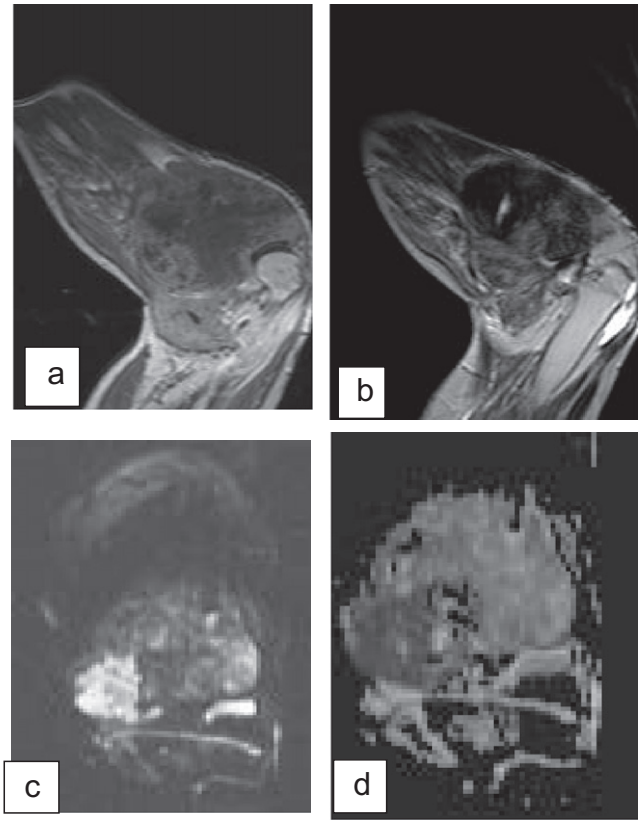

Fig. 8 Osteosarcoma of the forearm appears of low signal in sagittal T1WIs(a),heterogenos high signal in sagittal T2WIs (b)) Area of restriction in DWI(c,d) and ADC**.** ADC Value 0.9 ± 0.6.

the extracellular spaces in benign lesions as compared to that of malignant soft-tissue masses. These results were comparable to those of Nagata et al. (10) who stated that the size of the extracellular space is the most important component of the true diffusion measurement in soft-tissue tumors. A larger or less restricted extracellular space, allowing spin dephasing and loss of signal on diffusion-weighted images, is the most likely explanation for the increased diffusion of most benign soft-tissue tumors. Malignant soft-tissue tumors tend to have lower true diffusion measurements due to increased tumor cell packing in the majority of the malignant soft-tissue tumors, resulting in the restriction of Brownian motion in the extracellular space (11–12).

Our results revealed that ganglion cyst and cystic neurofibroma (Figs. 1 and 3) and juxtacortical enchnodroma (Fig. 2) had higher ADC values than those other benign soft-tissue lesions (Table 1). For malignant soft-tissue masses, the highest ADC value was seen in mesenchymal chondrosarcoma ($2.1 \pm 0.32 \times 10^{-3}$ mm^2/s) and liposarcoma (intermediate grade) (1.4 ± 0.21). These results were comparable with those of Nagata et al. (10) who stated that ADC values of myxomatous, cystic, and cartilaginous components are significantly higher than those of other tumors and even malignant cartilaginous tumor ADC values are higher than those of benign tumors.

Previous studies reported that not all benign soft-tissue tumors have a large extracellular space, and not all malignant soft-tissue tumors are more cellular than benign soft-tissue tumors. There was a considerable variation in true diffusion values within a group of liposarcomas and between the high- and low-grade myxofibrosarcomas. A possible explanation may be related to the various histologic subtypes and variation in the degree of tumor differentiation. Another explanation is that the ADC value is affected not only by cellularity but also by the amount and type of extracellular substance. Soft-tissue tumors, as opposed, for example, to brain tumors, are a highly heterogeneous entity as regards extracellular matrix. Some of the benign and malignant soft tissue tumoursshow such heterogeniety as may explain the overlapping of ADC values. (13–15).

In the current study the two patients with benign lesions, demonstrating very low ADC value (0.37 ± 0.05) similar to ADC values of malignant soft-tissue tumors, had aggressive fibromatosis (Fig. 4). This can be explained by the fact that, histologically, aggressive fibromatosis consists of relatively uniform spindle-shaped cells surrounded and separated from each other by collagen fibers. However, fibrosarcoma is also composed of a relatively uniform population of spindle cells, demonstrating variable anaplasia. Fibrosarcoma is differentiated from aggressive fibromatosis by increased collagen and the absence of atypia in the latter, which is beyond the reach of diffusion-weighted MRI (16).

Several techniques have been used to obtain diffusion-weighted MR images (13). We used a peripheral pulse-triggered conventional spin-echo sequence that corrects for, or minimizes the effects of vascular pulsation on MR images in the extremities, and which was described previously as a successful sequence for diffusion measurements (17,18). The main disadvantage of the spin-echo sequence is the long acquisition

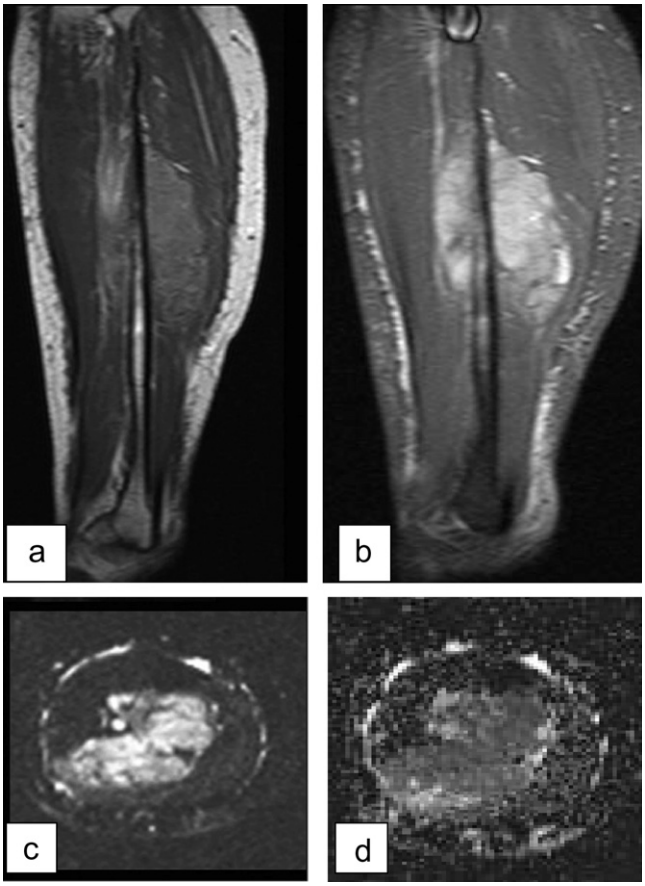

Fig. 9 Ewing's sarcoma of the fibula appears of low signal in sagittal T1WIs(a), contrast enhancement inpost contrast fat suppression sequence (b) . Restriction in DWI(c,d) and ADC. ADC Value 1.1 ± 0. 9

time, and the subsequent increased sensitivity to motion artifacts. Faster imaging sequences, such as echo planar techniques, are available and have been used for diffusion measurements in the human brain (17), hepatic lesions (19), and in the pelvis (20,21). Steady state free precession (SSFP) techniques have also been used in the musculoskeletal system for diffusion weighted MRI, with reported adequate image quality, SNRs, and relatively short acquisition times. The main disadvantages of the SSFP technique are the difficulties in quantifying diffusion, T2-contamination, and other confounding relaxation effects. Apparently, further studies are warranted to achieve faster diffusion-weighted spin-echo and/or EPI sequences with adequate image quality for diffusion measurements in the musculoskeletal system (22,23).

Limitations in our study were that lacking of some of the musculoskeletal tumor histologies, which make it difficult to know if our results are matching to all tumors or not, and also the difficulty in comparison of our results with those of others due to differences in imaging sequences and differences in *b*-values.

In conclusion, diffusion measurements of soft-tissue masses have potential as a non-invasive tool in the differentiation of benign and malignant soft-tissue lesions. It provides important additional information, but does not serve as a substitute for the routine MRI sequences. Further prospective studies with larger patient populations are required.

References

(1) Colagrande S, Carbone SF, Carusi LM, et al. Magnetic resonance diffusion-weighted imaging: extra neurological applications. J Radiol Med (Torino) 2006;111(3):392–419.
(2) Ross BD, Moffat BA, Lawrence TS, et al. Evaluation of cancer therapy using diffusion magnetic resonance imaging. J Mol Cancer Ther 2003;2(6):581–7.
(3) Costa Flavia M, Vianne Evandro M. Diffusion-weighted magnetic resonance imaging for the evaluation of musculoskeletal tumors. Magn Reson Imaging Clin North Am 2011;1(19):159–80.
(4) Gonzalez RG, Schaefer PW, Buonanno FS, et al. Diffusion-weighted MR imaging: diagnostic accuracy in patients imaged within 6 hours of stroke symptom onset. Radiology 1999;210: 155–62.
(5) Karonen JO, Liu Y, Vanninen RL, et al. Combined perfusion- and diffusion-weighted MR imaging in acute ischemic stroke during the 1st week: a longitudinal study. Radiology 2000;217: 886–94.
(6) Catherina SP, Patrik Kunz, Pancras CV, Antonie HM, et al. Diffusion-weighted MRI in characterization of soft tissue tumors. J Magn Reson Imaging 2002;15:302–7.
(7) Schnapauff Drik, Zeil Martin, Neiderhagen Manuel B, et al. Diffusion-weighted echo planar magnetic resonance imaging for the assessment of tumor cellularity in patient's with soft tissue sarcoma. J Magn Reson Imaging 2009;6(29):1355–9.
(8) Maier CF, Paran Y, Bendel P, Rutt BK, Degani H. Quantitative diffusion imaging in implanted human breast tumors. Magn Reson Med 1997;37:576–81.
(9) Baur A, Stabler A, Bruning R, et al. Diffusion-weighted MR imaging of bone marrow: differentiation of benign versus pathologic compression fractures. Radiology 1998;207:349–56.
(10) Nagata S, Nishimura H, Uchida M, Hayabuchi N. Usefulness of diffusion-weighted MRI in differentiating benign from malignant musculoskeletal tumors. Nippon Logaku Hoshasen Gakkai Zasshi (Japan) 2005;65(1):30–6.
(11) Taouli B, Vilgrain V, Dumont E, Dair JL, Fan B, Menu Y. Evaluation of the liver diffusion isotropy and characterization of the focal hepatic lesions with two single shot echoplannar MR imaging sequences:prospective study in 66patient. Radilogy 2003;226:71–8.
(12) Nakayama T, Yoshimitsu K, Irie H, Aibe H, Tajima T, Shinozaki K, et al. Usefulness of the calculated apparent diffusion coefficient value in the differential diagnosis of retroperitoneal masses. J Magn Reson Imaging 2004;20(4):735–42.
(13) Finarsdottir H, Karlsson M, Wejde J, Bauer HC. Diffusion-weighted MRI of soft tissue tumours. Eur Radiol 2004;14(6): 959–63.
(14) Dietrich Olaf, Raya José G, Sommer Julia, Deimling Michael, Reiser Maximilian F, Baur-Melnyk Andrea. A comparative evaluation of a RARE-based single-shot pulse sequence for diffusion-weighted MRI of musculoskeletal soft-tissue tumors. Eur Radiol 2005;15(4):772–83.
(15) Maeda M, Matsumine A, Kato H, et al. Soft-tissue tumors evaluated by line-scan diffusion-weighted imaging: influence of myxoid matrix on the apparent diffusion coefficient. J Magn Reson Imaging 2007;25(6):1199–204.
(16) Lasbleiz J, Askri A, Le Duff F, et al. Diffusion weighted MRI of spine tumors. J Radiol 2006;87(3):291–8.
(17) Yamada I, Aung W, Himeno Y, Nakagawa T, Shibuya H. Diffusion coefficients in abdominal organs and hepatic lesions: evaluation with intravoxel incoherent motion echo-planar MR imaging. Radiology 1999;210:617–23.
(18) Nonomura Y, Yasumoto M, Yoshimura R, et al. Relationship between bone marrow cellularity and apparent diffusion coefficient. J Magn Reson Imaging 2001;13:757–60.
(19) Baur A, Huber A, Arbogast S, et al. Diffusion-weighted imaging of tumor recurrencies and posttherapeutical soft-tissue changes in humans. Eur Radiol 2001;11:828–33.

(20) Ward R, Caruthers S, Yablon C, Blake M, DiMasi M, Eustace S. Analysis of diffusion changes in posttraumatic bone marrow using navigator-corrected diffusion gradients. AJR Am J Roentgenol 2000;174:731–4.
(21) Melhem ER, Itoh R, Jones L, Barker PB. Diffusion tensor MR imaging of the brain: effect of diffusion weighting on trace and anisotropy measurements. AJNR Am J Neuroradiol 2000;21:1813–20.
(22) Einarsdóttir H, Karlsson M, Wejde J, et al. Diffusion-weighted MRI of soft tissue tumours. J Eur Radiol 2004;14(6):959–63.
(23) Naganawa S, Kawai H, Fukatsu H, et al. Diffusion-weighted imaging of the liver: technical challenges and prospects for the future. J Magn Reson Med Sci 2005;4(4):175–86.